Research Article

URF PUBLISHERS
connect with research world

Journal of Petroleum & Chemical Engineering

https://urfpublishers.com/journal/petrochemical-engineering

Vol: 3 & Iss: 3

Analysis and Control of a Schizophrenia Model

Lakshmi N. Sridhar*

Chemical Engineering Department, University of Puerto Rico, Mayaguez, PR 00681, USA

Citation: Sridhar LN. Analysis and Control of a Schizophrenia Model. *J Petro Chem Eng* 2025;3(3):174-179.

Received: 22 September, 2025; **Accepted:** 24 September, 2025; **Published:** 26 September, 2025

***Corresponding author:** Lakshmi N. Sridhar, Chemical Engineering Department, University of Puerto Rico, Mayaguez, PR 00681, USA, Email: lakshmin.sridhar@upr.edu

ABSTRACT

Schizophrenia is a very debilitating illness that affects many people in the world and is caused by abnormal neural activities in the brain. The dynamics of this neural activity in neurons is very complex and nonlinear and it is important to understand the nonlinearity and develop strategies to control the neurons as effectively as possible. In this work, bifurcation analysis and multiobjective nonlinear model predictive control is performed on a Schizophrenia Model. Bifurcation analysis is a powerful mathematical tool used to deal with the nonlinear dynamics of any process. Several factors must be considered and multiple objectives must be met simultaneously. The MATLAB program MATCONT was used to perform the bifurcation analysis. The MNLMPC calculations were performed using the optimization language PYOMO in conjunction with the state-of-the-art global optimization solvers IPOPT and BARON. The bifurcation analysis revealed the existence of a Hopf bifurcation point and a limit point. The MNLMC converged to the utopia solution. The Hopf bifurcation point, which causes an unwanted limit cycle, is eliminated using an activation factor involving the tanh function. The limit points (which cause multiple steady-state solutions from a singular point) are very beneficial because they enable the Multiobjective nonlinear model predictive control calculations to converge to the Utopia point (the best possible solution) in the model.

Keywords: Bifurcation; Optimization; Control; Neuron; Schizophrenia

Background

Gothelf, et al.[1], provided evidence for the involvement of the hippocampus in the pathophysiology of schizophrenia. Harrison, et al.[2] discussed Schizophrenia genes, gene expression and neuropathology on the matter of their convergence. Jalili, et al.[3], describe the dysconnection topography in schizophrenia revealed with state-space analysis of EEG. Rolls, et al.[4] discussed the various computational models of schizophrenia and dopamine modulation in the prefrontal cortex. Fornito, et al.[5] describe the anatomical abnormalities of the anterior cingulate cortex in schizophrenia. Heckers[6] describe the neuroimaging studies of the hippocampus in schizophrenia. Knyazeva, et al.[7] discuss the alpha rhythm and hypofrontality in schizophrenia. Lynall, et al.[8] discuss the functional connectivity and brain networks in schizophrenia. Camchong, et al.[9], researched the altered functional and anatomical connectivity in schizophrenia. Kanahara, et al.[10] studied the orbitofrontal cortex abnormality and deficit schizophrenia. Cui, et al.[11] described the anterior cingulate cortex-related connectivity in first-episode schizophrenia and performed a spectral dynamic causal modeling study with functional magnetic resonance imaging. Duan, et al.[12] performed a longitudinal study on intrinsic connectivity of hippocampus associated with positive symptom in first-episode schizophrenia. Guo, et al.[13], describe the abnormal causal connectivity by structural deficits in first-episode, drug-naive schizophrenia at rest. Sarpal, et al.[14] researched the antipsychotic treatment and functional connectivity of the striatum in first-episode schizophrenia. Sheffield, et al.[15] discuss cognition and resting-state functional connectivity in schizophrenia. Lin, et al.[16] discuss the functional dysconnectivity of the limbic loop of front striatal circuits in first-episode, treatment-naive schizophrenia. Ahn[17] targeted reduced neural oscillations in patients with schizophrenia by transcranial alternating current stimulation. Szalisznyó, et al.[18] researched the dynamics in co-morbid schizophrenia and OCD using a computational approach. Hua, et al.[19] investigated the disrupted pathways from limbic areas to thalamus in schizophrenia highlighted by whole-brain resting-state effective connectivity analysis. Gangadin[20] worked on the reduced resting state functional connectivity in the hippocampus-midbrain-striatum network of schizophrenia patients. Chen, et al.[21] performed a bifurcation analysis of brain connectivity and regulated neural oscillations in Schizophrenia. In this work, bifurcation analysis and multiobjective nonlinear model predictive control is performed on the Schizophrenia Model[21]. The paper is organized as follows. First, the model equations are presented, followed by a discussion of the numerical techniques involving bifurcation analysis and multiobjective nonlinear model predictive control (MNLMPC). The results and discussion are then presented, followed by the conclusions.

Model Equations[21]

In this model, the variables $cv, ov, pv, av, tv, vv, dv, hv, \delta,$ represent the neuronal populations in the anterior cingulate cortex orbitofrontal cortex, dorsolateral prefrontal cortex, amygdala, thalamus, ventral striatum, dorsal striatum, hippocampus and VTA/substantia nigra pars.

The model equations are

$$\frac{d(cv)}{dt} = -lp(cv) + mp(ov+av+tv) + vp(pv) + h1p(hv) + \frac{1}{\left(exp\left(\left(-\mu(cv-\delta)\right)+0.5\right)\right)}$$

$$\frac{d(ov)}{dt} = -ip(ov) + mp(av+tv) + h1p(hv) + \frac{1}{\left(exp\left(\left(-\mu(ov-\delta)\right)+0.5\right)\right)}$$

$$\frac{d(pv)}{dt} = -np(pv) + mp(ov+tv) + h2p(hv) + \frac{1}{\left(exp\left(\left(-\mu(pv-\delta)\right)+0.5\right)\right)}$$

$$\frac{d(av)}{dt} = -ap(av) + mp(hv+tv+delv) - rp(ov+cv) + \frac{1}{\left(exp\left(\left(-\mu(av-\delta)\right)+0.5\right)\right)}$$

$$\frac{d(tv)}{dt} = -np(tv) + mp(ov+cv+pv+av+dv+hv) + 1/\left(exp\left(\left(-\mu(tv-\delta)\right)+0.5\right)\right)$$

$$\frac{d(vv)}{dt} = -np(vv) + yp(cv) + b1p(ov) + b2p(av) + mp(tv) + jp(dv) - gp(\delta) +$$
$$\frac{1}{\left(exp\left(\left(-\mu(vv-\delta)\right)+0.5\right)\right)}$$

$$d(dv) = -np(dv) + yp(cv) + b1p(ov) + b2p(av) + mp(tv+pv) + kp(vv) - gp(\delta) +$$
$$\frac{1}{\left(exp\left(\left(-mu(dv-\delta)\right)+0.5\right)\right)}$$

$$d(hv) = -np(hv) + mp(tv+cv+ov+av) + ep(pv) + \frac{1}{\left(exp\left(\left(-\mu(hv-\delta)\right)+0.5\right)\right)}$$

$$\frac{d(\delta)}{dt} = -np(\delta) + mp(tv+cv+ov+av+hv)$$

The base parameter values are

$$up = 0.1; vp = 1.5; jp = 1; kp = 1; ep = 0.3; \; yp = 0.2; b1p = 1; b2p = 1; gp = 0.7;$$
$$np = 1.4; lp = 3; ip = 14; ap = 1.4; \; mp = 0.5; rp = 2; h1p = 0.7; h2p = 0.6; \; \mu = 0.1;$$

lp and *ap* are the bifurcation parameters and the control values.

Bifurcation Analysis

The MATLAB software MATCONT is used to perform the bifurcation calculations. Bifurcation analysis deals with multiple steady-states and limit cycles. Multiple steady states occur because of the existence of branch and limit points. Hopf bifurcation points cause limit cycles. A commonly used MATLAB program that locates limit points, branch points and Hopf bifurcation points is MATCONT[22,23]. This program detects Limit points (LP), branch points (BP) and Hopf bifurcation points(H) for an ODE system.

$$\frac{dx}{dt} = f(x, \alpha)$$

$x \in R^n$ Let the bifurcation parameter be α . Since the gradient is orthogonal to the tangent vector,

The tangent plane at any point $w = [w_1, w_2, w_3, w_4, ...w_{n+1}]$ must satisfy

$$Aw = 0$$

Where A is

$$A = [\partial f / \partial x \quad | \partial f / \partial \alpha]$$

where $\partial f / \partial x$ is the Jacobian matrix. For both limit and branch points, the Jacobian matrix $J = [\partial f / \partial x]$ must be singular.

For a limit point, there is only one tangent at the point of singularity. At this singular point, there is a single non-zero vector, y, where Jy=0. This vector is of dimension n. Since there is only one tangent the vector

$y = (y_1, y_2, y_3, y_4, ...y_n)$ must align with $\hat{w} = (w_1, w_2, w_3, w_4, ...w_n)$. Since

$$J\hat{w} = Aw = 0$$

the n+1 th component of the tangent vector w_{n+1} = 0 at a limit point (LP).

For a branch point, there must exist two tangents at the singularity. Let the two tangents be z and w. This implies that

$$Az = 0$$
$$Aw = 0$$

Consider a vector v that is orthogonal to one of the tangents (say w). v can be expressed as a linear combination of z and w ($v = \alpha z + \beta w$). Since $Az = Aw = 0$; $Av = 0$ and since w and v are orthogonal, $w^T v = 0$. Hence $Bv = \begin{bmatrix} A \\ w^T \end{bmatrix} v = 0$ which implies that B is singular.

Hence, for a branch point (BP) the matrix $B = \begin{bmatrix} A \\ w^T \end{bmatrix}$ must be singular.

At a Hopf bifurcation point,

$$\det(2 f_x(x, \alpha) @ I_n) = 0$$

@ indicates the bialternate product while I_n is the n-square identity matrix. Hopf bifurcations cause limit cycles and should be eliminated because limit cycles make optimization and control tasks very difficult. More details can be found in Kuznetsov[24-26].

Hopf bifurcations cause limit cycles. The tanh activation function (where a control value u is replaced by) $(u \tanh u / \varepsilon)$ is used to eliminate spikes in the optimal control profiles[27-30]. Sridhar[31] explained with several examples how the activation factor involving the tanh function also eliminates the Hopf bifurcation points. This was because the tanh function increases the oscillation time period in the limit cycle.

Multiobjective Nonlinear Model Predictive Control(MNLMPC)

The rigorous multiobjective nonlinear model predictive control (MNLMPC) method developed by Flores Tlacuahuaz, et al.[32] was used.

Consider a problem where the variables $\sum_{t_{i=0}}^{t_i=t_f} q_j(t_i)$ (j=1, 2..n) have to be optimized simultaneously for a dynamic problem

$$\frac{dx}{dt} = F(x,u)$$

t_f being the final time value and n the total number of objective variables and u the control parameter. The single objective optimal control problem is solved individually optimizing each of the variables $\sum_{t_{i=0}}^{t_i=t_f} q_j(t_i)$ The optimization of $\sum_{t_{i=0}}^{t_i=t_f} q_j(t_i)$ will lead to the values q_j^*. Then, the multiobjective optimal control (MOOC) problem that will be solved is

$$\min(\sum_{j=1}^{n}(\sum_{t_{i=0}}^{t_i=t_f} q_j(t_i) - q_j^*))^2$$

$$subject\ to\ \frac{dx}{dt} = F(x,u);$$

This will provide the values of u at various times. The first obtained control value of u is implemented and the rest are discarded. This procedure is repeated until the implemented and the first obtained control values are the same or if the Utopia point where ($\sum_{t_{i=0}}^{t_i=t_f} q_j(t_i) = q_j^*$ for all j) is obtained.

Pyomo[33] is used for these calculations. Here, the differential equations are converted to a Nonlinear Program (NLP) using the orthogonal collocation method The NLP is solved using IPOPT[34] and confirmed as a global solution with BARON[35].

The steps of the algorithm are as follows

Optimize $\sum_{t_{i=0}}^{t_i=t_f} q_j(t_i)$ and obtain q_j^*.

Minimize $(\sum_{j=1}^{n}(\sum_{t_{i=0}}^{t_i=t_f} q_j(t_i) - q_j^*))^2$ and get the control values at various times.

Implement the first obtained control values

Repeat steps 1 to 3 until there is an insignificant difference between the implemented and the first obtained value of the control variables or if the Utopia point is achieved. The Utopia point is when $\sum_{t_{i=0}}^{t_i=t_f} q_j(t_i) = q_j^*$ for all j.

Sridhar[36] demonstrated that when the bifurcation analysis revealed the presence of limit and branch points tthe MNLMPC calculations to converge to the Utopia solution . For this, the singularity condition, caused by the presence of the limit or branch points was imposed on the co-state equation[37]. If the minimization of q_1 lead to the value q_1^* and the minimization of q_2 lead to the value q_2^* The MNLPMC calculations will minimize the function $(q_1 - q_1^*)^2 + (q_2 - q_2^*)^2$. The multiobjective optimal control problem is

$$\min \quad (q_1 - q_1^*)^2 + (q_2 - q_2^*)^2 \quad subject\ to\ \frac{dx}{dt} = F(x,u)$$

Differentiating the objective function results in

$$\frac{d}{dx_i}((q_1 - q_1^*)^2 + (q_2 - q_2^*)^2) = 2(q_1 - q_1^*)\frac{d}{dx_i}(q_1 - q_1^*) + 2(q_2 - q_2^*)\frac{d}{dx_i}(q_2 - q_2^*)$$

The Utopia point requires that both $(q_1 - q_1^*)$ and $(q_2 - q_2^*)$ are zero. Hence

$$\frac{d}{dx_i}((q_1 - q_1^*)^2 + (q_2 - q_2^*)^2) = 0$$

The optimal control co-state equation is

$$\frac{d}{dt}(\lambda_i) = -\frac{d}{dx_i}((q_1 - q_1^*)^2 + (q_2 - q_2^*)^2) - f_x\lambda_i; \quad \lambda_i(t_f) = 0$$

λ_i is the Lagrangian multiplier. t_f is the final time. The first term in this equation is 0 and hence

$$\frac{d}{dt}(\lambda_i) = -f_x\lambda_i; \lambda_i(t_f) = 0$$

At a limit or a branch point, for the set of ODE $\frac{dx}{dt} = f(x,u)$ f_x is singular. Hence there are two different vectors-values for $[\lambda_i]$ where $\frac{d}{dt}(\lambda_i) > 0$ and $\frac{d}{dt}(\lambda_i) < 0$. In between there is a vector $[\lambda_i]$ where $\frac{d}{dt}(\lambda_i) = 0$. This coupled with the boundary condition $\lambda_i(t_f) = 0$ will lead to $[\lambda_i] = 0$ This makes the problem an unconstrained optimization problem and the optimal solution is the Utopia solution.

Results and Discussion

When bifurcation analysis was performed with ap as the bifurcation parameter a Hopf bifurcation point was found at $(cv, ov, pv, av, tv, vv, dv, hv, \delta, ap)$ values (1.249626

0.098359 1.502862 -1.431220 1.352159 -0.447452 -0.127160 1.223140 0.890023 0.337072) (Curve AB in **Figure 1a**). When the bifurcation parameter was modified to aptanh(ap)/750, the Hopf bifurcation point disappears (curve CD in **Figure 1b**). The tanh activation factor eliminates the Hopf bifurcation point, validating the hypothesis of Sridhar[31]. The limit cycle caused by this Hopf bifurcation point is seen in Fig. 1b. A limit point occurred for (ap as the bifurcation parameter) at $(cv, ov, pv, av, tv, vv, dv, hv, \delta, ap)$ values (72.271699 7.366376 73.272255 -7.053591 103.239848 45.139939 60.414400 78.622854 90.873995 3.247675) **(Figure 1c)**.

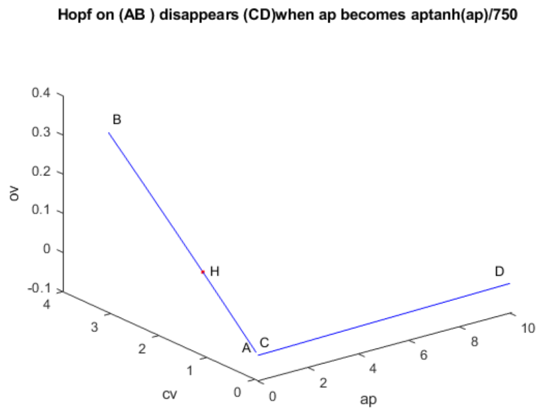

Figure 1a: Hopf on curve AB disappears (CD) when ap is modified to ap(tanh(ap))/750.

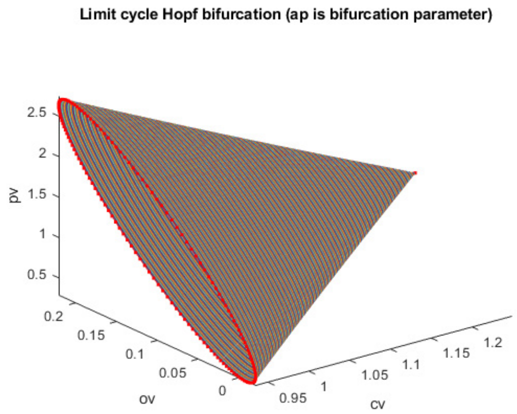

Figure 1b: Limit cycle for Hopf bifurcation (ap is the bifurcation parameter).

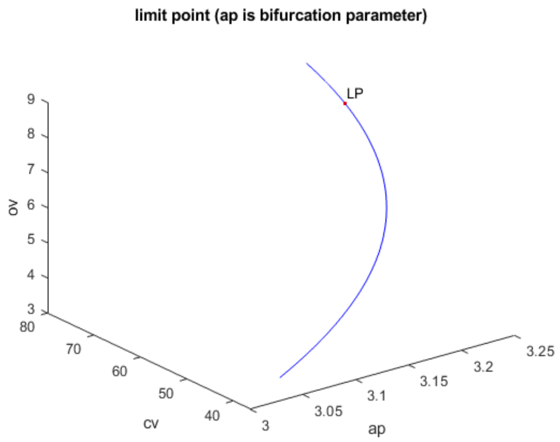

Figure 1c: (limit point when ap is bifurcation parameter).

When bifurcation analysis was performed with lp as the bifurcation parameter a Hopf bifurcation point was found at $(cv, ov, pv, av, tv, vv, dv, hv, \delta, lp)$ values (1.986754 0.040225 1.048587 -1.832801 0.513919 -2.157130 -1.934346 0.925913 0.583575 1.147394) (Curve AB in **Figure 1d**). When the bifurcation parameter was modified to lptanh(lp)/30, the Hopf bifurcation point disappears (curve CD in **Figure 1d**). The tanh activation factor eliminates the Hopf bifurcation point, validating the hypothesis of Sridhar[31] **(Figure 1e)**. A limit point occurred for (lp as the bifurcation parameter) at $(cv, ov, pv, av, tv, vv, dv, hv, \delta, lp)$ values (49.965991 5.968514 58.519954 -2.734106 83.636483 44.294984 56.529178 61.581545 70.863724 3.490324) **(Figure 1f)**.

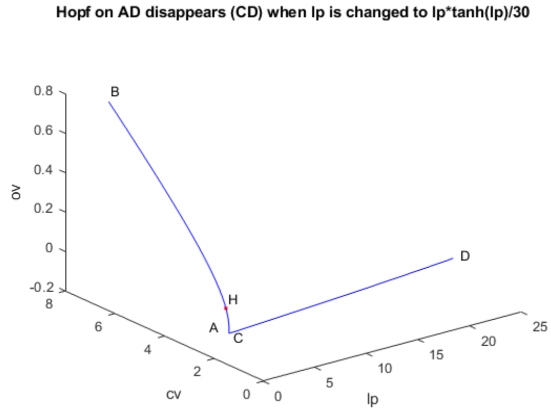

Figure 1d: Hopf on curve AB disappears (CD) when ap is modified to lp(tanh(lp))/30.

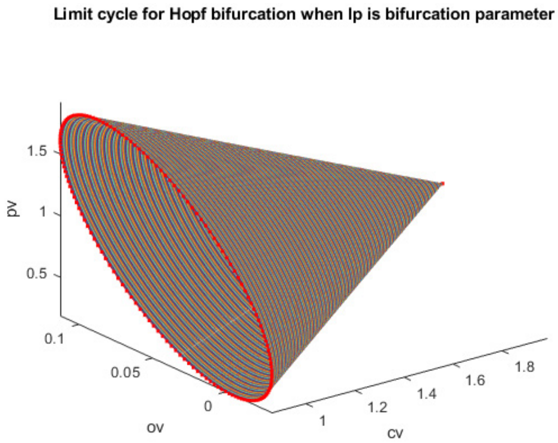

Figure 1e: Limit cycle for Hopf bifurcation (lp is the bifurcation parameter).

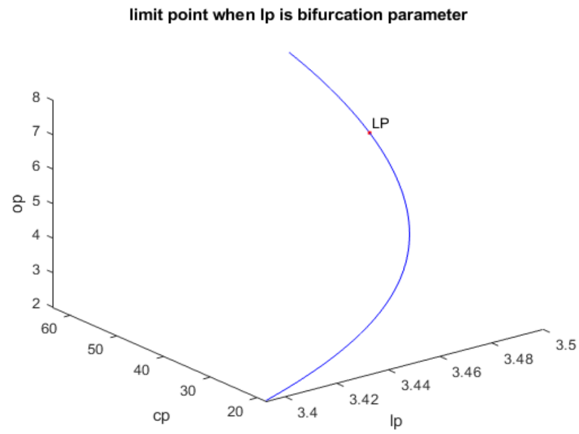

Figure 1f: (limit point when lp is the bifurcation parameter).

For the MNLMPC *ap* and *lp* are the control parameters and $\sum_{t_i=0}^{t_i=t_f} cv(t_i), \sum_{t_i=0}^{t_i=t_f} vv(t_i) \sum_{t_i=0}^{t_i=t_f} vv(t_i)$ were maximized individually and each of them led to a value of 300. The overall optimal control problem will involve the minimization of $(\sum_{t_i=0}^{t_i=t_f} cv(t_i)-300)^2+(\sum_{t_i=0}^{t_i=t_f} vv(t_i)-300)^2+(\sum_{t_i=0}^{t_i=t_f} tv(t_i)-300)^2$ was minimized subject to the equations governing the model. This led to a value of zero (the Utopia point). The MNLMPC values of the control variables, *ap* and lp were 4.925 and 6.34. The MNLMPC profiles are shown in **(Figures 2a-2d)**. The control profiles of *ap* and *lp* exhibits noise and this was remedied using the Savitzky-Golay filter to produce the smooth profiles apsg lpsg The presence of the limit points is beneficial because it allows the MNLMPC calculations to attain the Utopia solution, validating the analysis of Sridhar[36].

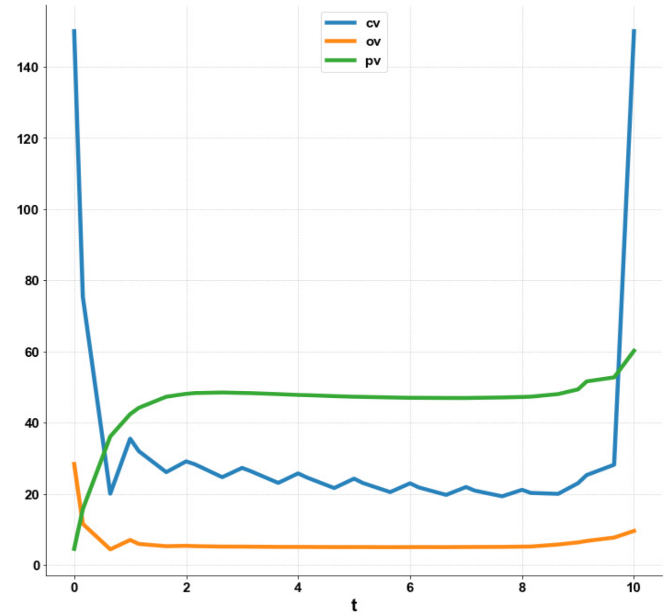

Figure 2a: MNLMPC (cv, ov, tv profiles).

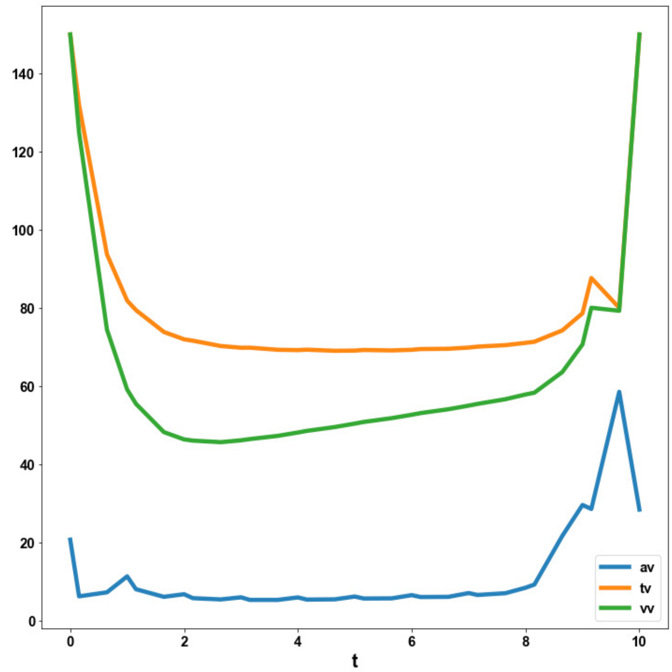

Figure 2b: (av tv vv profiles).

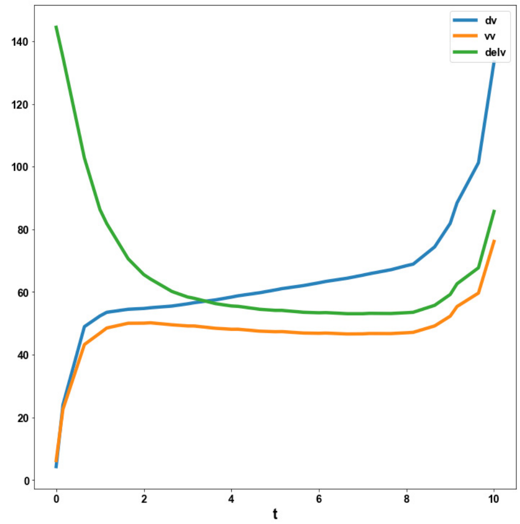

Figure 2c: (dv vv delv profiles).

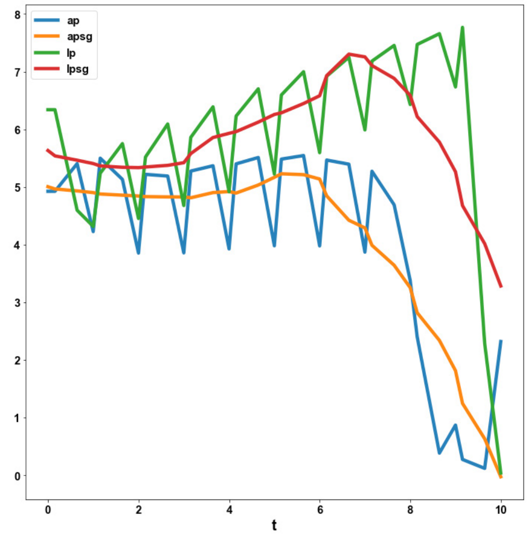

Figure 2d: (ap apsg lp lpsg profiles).

Conclusions

Bifurcation analysis and multiobjective nonlinear control (MNLMPC) studies on a Schizophrenia Model. The bifurcation analysis revealed the existence of Hopf bifurcation points and limit points . The Hopf bifurcation point, which causes an unwanted limit cycle, is eliminated using an activation factor involving the tanh function. The limit points (which cause multiple steady-state solutions from a singular point) are very beneficial because they enable the Multiobjective nonlinear model predictive control calculations to converge to the Utopia point (the best possible solution) in the models. A combination of bifurcation analysis and Multiobjective Nonlinear Model Predictive Control(MNLMPC) for a Schizophrenia Model is the main contribution of this paper.

Data Availability Statement

All data used is presented in the paper.

Conflict of Interest

The author, Dr. Lakshmi N Sridhar has no conflict of interest.

Acknowledgement

Dr. Sridhar thanks Dr. Carlos Ramirez and Dr. Suleiman for encouraging him to write single-author papers

References

1. Gothelf D, Soreni N, Nachman RP, Tyano S, Hiss Y. Evidence for the involvement of the hippocampus in the pathophysiology of schizophrenia. Eur Neuropsychopharmacol 2000;10:389-395.
2. Harrison PJ, Weinberger DR. Schizophrenia genes, gene expression and neuropathology: on the matter of their convergence. Mol Psychiatr 2005;10:40-68.
3. Jalili M, Lavoie S, Deppen P, et al. Dysconnection topography in schizophrenia revealed with state-space analysis of EEG. Plos One 2007;2:1059.
4. Rolls ET, Loh M, Deco G, Winterer G. Computational models of schizophrenia and dopamine modulation in the prefrontal cortex. Nat Rev Neurosci 2008;9:696-709.
5. Fornito A, Yucel M, Dean B, Wood SJ, Pantelis C. Anatomical abnormalities of the anterior cingulate cortex in schizophrenia: Bridging the gap between neuroimaging and neuropathology. Schizophrenia Bull 2009;35:973-993.
6. Heckers S. Neuroimaging studies of the hippocampus in schizophrenia. Hippocampus 2010;11:520-528.
7. Knyazeva MG, Jalili M, Meuli R, et al. Alpha rhythm and hypofrontality in schizophrenia. Acta Psychiat. Scand 2010;118:188-199.
8. Lynall ME, Bassett DS, Kerwin R, McKenna PJ, Kitzbichler M, Müller U, Bullmore E. Functional connectivity and brain networks in schizophrenia. J Neurosci 2010;30:9477-9487.
9. Camchong J, Macdonald AW, Bell C, Mueller BA, Lim KO. Altered functional and anatomical connectivity in schizophrenia. Schizophrenia Bull 2011;37:640-650.
10. Kanahara N, Sekine Y, Haraguchi T, et al. Orbitofrontal cortex abnormality and deficit schizophrenia. Schizophr Res 2013;143:246-252.
11. Cui LB, Liu J, Wang LX, et al. Anterior cingulate cortex-related connectivity in first-episode schizophrenia: a spectral dynamic causal modeling study with functional magnetic resonance imaging. Front Hum Neurosci 2015;9:589.
12. Duan HF, Gan JL, Yang JM, et al. A longitudinal study on intrinsic connectivity of hippocampus associated with positive symptom in first-episode schizophrenia. Behav Brain Res 2015;283:78-86.
13. Guo WB, Liu F, Liu JR, et al. Abnormal causal connectivity by structural deficits in first-episode, drug-naive schizophrenia at rest. Schizophr Bull 2015;41:57-65.
14. Sarpal DK, Robinson DG, Lencz T, et al. Antipsychotic treatment and functional connectivity of the striatum in first-episode schizophrenia. JAMA Psychiat 2015;72:5-13.
15. Sheffield JM, Barch DM. Cognition and resting-state functional connectivity in schizophrenia. Neurosci Biobehav R 2016;61:108-120.
16. Lin P, Wang XS, Zhang B, et al. Functional dysconnectivity of the limbic loop of frontostriatal circuits in first-episode, treatment-naive schizophrenia. Hum Brain Mapp 2018;39:747-757.
17. Ahn S, Mellin JM, Alagapan S, et al. Targeting reduced neural oscillations in patients with schizophrenia by transcranial alternating current stimulation. Neuroimage 2019;186:126-136.
18. Szalisznyó K, Silverstein DN, Tóth J. Neural dynamics in co-morbid schizophrenia and OCD: A computational approach. J Theor Biol 2019;473:80-94.
19. Hua MH, Peng YM, Zhou Y, Qin W, Yu CS, Liang M. Disrupted pathways from limbic areas to thalamus in schizophrenia highlighted by whole-brain resting-state effective connectivity analysis. Prog Neuro-Psychoph 2019;99:109837.
20. Gangadin SS, Cahn W, Scheewe TW, Pol HEH, Bossong G. Reduced resting state functional connectivity in the hippocampus-midbrain-striatum network of schizophrenia patients. J Psychiatr Res 2021;138:83-88.
21. Yaqian C, Bilal GM, Yanmei K. Bifurcation Analysis of Brain Connectivity Regulated Neural Oscillations in Schizophrenia. Int J Bifurcation and Chaos 2022;2250167.
22. Dhooge A, Govearts W, Kuznetsov AY. MATCONT: A Matlab package for numerical bifurcation analysis of ODEs. ACM transactions on Mathematical software 2003;29(2):141-164.
23. Dhooge A, Govaerts W, Kuznetsov YA, Mestrom W, Riet AM. CL_MATCONT. A continuation toolbox in Matlab 2004.
24. Kuznetsov YA. Elements of applied bifurcation theory. Springer, NY 1998.
25. Kuznetsov YA. Five lectures on numerical bifurcation analysis. Utrecht University, NL 2009.
26. Govaerts WJF. Numerical Methods for Bifurcations of Dynamical Equilibria. SIAM 2000.
27. Dubey SR, Singh SK, Chaudhuri BB. Activation functions in deep learning: A comprehensive survey and benchmark. Neurocomputing 2022;503:92-108.
28. Kamalov AF, Safaraliev NM, Cherukuri AK, Zgheib R. Comparative analysis of activation functions in neural networks. 28th IEEE Int Conf Electronics, Circuits and Systems (ICECS) 2021:1-6.
29. Szandała T. Review and Comparison of Commonly Used Activation Functions for Deep Neural Networks. ArXiv 2020.
30. Sridhar LN. Bifurcation Analysis and Optimal Control of the Tumor Macrophage Interactions. Biomed J Sci & Tech Res 2023;53(5).
31. Sridhar LN. Elimination of oscillation causing Hopf bifurcations in engineering problems. J App Math 2024;2(4):1826.
32. Flores-Tlacuahuac A. Pilar Morales and Martin Riveral Toledo. Multiobjective Nonlinear model predictive control of a class of chemical reactors. I & EC research 2012:5891-5899.
33. William HE, Laird CD, Watson JP, et al. Pyomo - Optimization Modeling in Python Second Edition 67.
34. Wächter A, Biegler L. On the implementation of an interior-point filter line-search algorithm for large-scale nonlinear programming. Math Program 2006;106:25-57.
35. Tawarmalani M, Sahinidis NV. A polyhedral branch-and-cut approach to global optimization. Mathematical Programming 2005;103(2):225-249.
36. Sridhar LN. Coupling Bifurcation Analysis and Multiobjective Nonlinear Model Predictive Control. Austin Chem Eng 2024;10(3):1107.
37. Upreti SR. Optimal control for chemical engineers. Taylor and Francis 2013.